Progress In Electromagnetics Research C, Vol. 107, 81–96, 2021

A Compact U-Shaped UWB-MIMO Antenna with Novel Complementary Modified Minkowski Fractal for Isolation Enhancement

Rohit Gurjar[1], Dharmendra K. Upadhyay[2], Binod K. Kanaujia[3], and Amit Kumar[4, *]

Abstract—A compact U-shaped ultra-wideband (UWB) multiple-input-multiple-output (MIMO) antenna with novel complementary modified Minkowski fractal (CMMF) for isolation enhancement is proposed. This antenna consists of two identical U-shaped monopole elements, a novel CMMF and a slot in the bottom of the ground plane for the isolation enhancement. The novel CMMF is designed by a technique iterated function system (IFS). The overall dimension of this compact antenna is $22 \times 28\,\text{mm}^2$. The impedance bandwidth of this antenna is 10.35 GHz, ranging from 3.06 GHz to 13.41 GHz. The minimum isolation is 17.07 dB for the operating frequency range and 18.4 dB for the UWB frequency range 3.1 to 10.6 GHz. The diversity parameters are also determined for the proposed MIMO antenna, and all are found satisfactory. The proposed MIMO antenna is fabricated, and its prototype measured results are found in good agreement with the simulated ones.

1. INTRODUCTION

Federal Communications Commission (FCC) legalized making use of unlicensed frequency bandwidth ranging from 3.1 to 10.6 GHz with a power limit of -41.3 dBm/MHz for commercial communication objective [1]. It has created interest among researchers to utilize ultra-wideband (UWB) technology for short-range applications with low power limits and high data rates. However, there is a multi-path fading problem in UWB systems. This drawback can be overcome by the introduction of multiple-input-multiple-output (MIMO) techniques in UWB systems [2]. In MIMO systems, multiple antennas are used at both the receiver and transmitter to improve the channel capacity and reliability of communication [3, 4]. Since there are multiple antenna elements in a MIMO system, it is a challenge to design a compact MIMO antenna by keeping mutual coupling as low as possible. In literature, the mutual coupling is reduced by several techniques such as defected ground structures (DGSs), antenna elements orientation, parasitic elements, neutralization lines, decoupling networks, and meta-materials [5]. Fractal structures can be used to design compact MIMO antennas with low mutual coupling due to their unique properties [6–9]. The effective electrical length of antenna elements can be increased by the application of fractal geometry due to its space-filling property in a given compact area [10]. Fractal shaped DGSs can be used to reduce the mutual coupling between adjacent elements of MIMO antennas [11, 12]. In this article, a novel complementary modified Minkowski fractal (CMMF) is loaded to enhance the isolation between the U-shaped radiating elements of a UWB-MIMO antenna. This novel fractal structure is designed by using the iterated function system (IFS) method.

Received 18 September 2020, Accepted 20 November 2020, Scheduled 30 November 2020
* Corresponding author: Amit Kumar (amit.kumarc210@gmail.com).
[1] Department of Electronics and Communication Engineering, Faculty of Technology, University of Delhi, New Delhi, Delhi 110021, India. [2] Division of Electronics and Communication Engineering, Netaji Subhas University of Technology, New Delhi, Delhi 110078, India. [3] School of Computational and Integrative Sciences, Jawaharlal Nehru University, New Delhi, Delhi 110067, India.
[4] Department of Electrical and Electronics Engineering, Darbhanga College of Engineering, Darbhanga, Bihar 846005, India.

Many fractal UWB-MIMO antennas have been reported in the past [13–22]. Koch [13], self-similar [14], complementary Sierpinski gasket [15], modified Sierpinski carpet [16], and hybrid Sierpinski Koch [17] shaped two-element fractal monopole UWB-MIMO antennas are reported in [13–17]. Koch [18], hexagonal molecule shaped [19], and Sierpinski Knopp [20] shaped four-element fractal monopole UWB-MIMO antennas are reported in [18–20]. In the above-reported MIMO antennas, fractal structures are used on patch sides to achieve miniaturization and wideband characteristics. In [21, 22], the Hilbert fractal shaped [21] and modified Minkowski fractal shaped [22] defects are introduced in the ground plane for the enhancement of isolation of UWB-MIMO antennas. The overall size of the smallest antenna is 720 mm^2 out of all above mentioned fractal UWB-MIMO antennas, as mentioned in Table 1.

Table 1. Comparison table of our proposed antenna with the reported fractal UWB-MIMO antennas.

S. No.	No. of elements	Fractal geometry	Size (mm^2)	Frequency band (GHz)	Min. isolation (dB)	Ref. No.
1	2	Koch fractal	$40 \times 25 = 1000$	3.3–10.8	15	[13]
2	2	Self-similar fractal	$24 \times 32 = 768$	3.1–12.5	16	[14]
3	2	Complementary Sierpinski gasket fractal	$41 \times 99.4 = 4075.4$	4.3–11.6	15.8	[15]
4	2	Modified Sierpinski carpet fractal	$24 \times 30 = 720$	3.0–12.6	16.3	[16]
5	2	Hybrid Sierpinski Koch fractal	$20 \times 40 = 800$	2.5–11	20	[17]
6	4	Koch fractal	$45 \times 45 = 2025$	2.0–10.6	17	[18]
7	4	Hexagonal molecule-shaped fractal	$40 \times 40 = 1600$	3.1–10.6	20	[19]
8	4	Sierpinski Knopp fractal	$40 \times 40 = 1600$	2.6–10.6	20	[20]
9	2	Hilbert fractal	$30 \times 41 = 1230$	2.2–11	20	[21]
10	2	Modified Minkowski fractal	$26.75 \times 41.5 = 1110.12$	3.1–11.5	19	[22]
11	2	Complementary Modified Minkowski fractal	$22 \times 28 = 616$	3.06–13.41	17.07	Proposed

In this article, a novel CMMF structure is used in the ground plane for isolation enhancement. It contains two U-shaped radiating elements with an operating frequency range from 3.06 to 13.41 GHz. Unlike many, we have used the fractal structure in the ground plane for better isolation and miniaturization. A novel CMMF is loaded on a T-shaped ground stub to enhance isolation up to 17.07 dB. This antenna is compared with the above mentioned reported antennas in Table 1. It is observed that the proposed antenna is the smallest in size and has considerable isolation as compared to the mentioned fractal UWB-MIMO antennas in Table 1.

2. ANTENNA DESIGN

2.1. Antenna Configuration

The geometry of the proposed two-element MIMO antenna is illustrated in Figure 1. The proposed MIMO antenna contains two identical U-shaped radiating elements with a novel CMMF for isolation enhancement, and it is fabricated on an FR-4 dielectric substrate (dielectric constant is 4.3, loss tangent 0.025, and thickness 0.8 mm). The dimensions of this antenna are listed in Table 2. The overall size of this compact MIMO antenna is $22 \times 28\,\text{mm}^2$, and its prototype image is shown in Figure 9. The two identical U-shaped monopole structures are considered for miniaturized UWB-MIMO antenna design, and their dimensions are optimized to fulfil the UWB operating frequency requirements.

Table 2. Proposed antenna parameters dimensions (Unit: mm).

Parameters	**L**	$\mathbf{L}_P$	$\mathbf{L}_F$	$\mathbf{L}_{G1}$	$\mathbf{L}_{G2}$	$\mathbf{L}_{S1}$	$\mathbf{L}_{S2}$	$\mathbf{L}_{S3}$	$\mathbf{L}_{S4}$	$\mathbf{L}_{S5}$
Dimensions (mm)	22	7	11.9	10.5	1.5	3	2	2	2.5	1
Parameters	**W**	$\mathbf{W}_P$	$\mathbf{W}_F$	$\mathbf{W}_{G1}$	$\mathbf{W}_{G2}$	$\mathbf{W}_{S1}$	$\mathbf{W}_{S2}$	$\mathbf{W}_{S3}$	$\mathbf{W}_{S4}$	**A**
Dimensions (mm)	28	9.5	1.2	5.4	7.75	8	0.5	2.5	0.5	1.5

In our proposed MIMO antenna, we designed U-shape from a rectangular shape by cutting a slot in a rectangular-shaped monopole element. The evolution of U-shaped monopole element is shown in Figure 2. The fundamental lower resonant frequency of the rectangular-shaped monopole element (as shown in Figure 2(a)) could be approximated by the given equation below [23].

$$f_r = \frac{14.4}{l_1 + l_2 + g + \dfrac{A_1}{2\pi l_1\sqrt{\varepsilon_{re}}} + \dfrac{A_2}{2\pi l_2\sqrt{\varepsilon_{re}}}} \tag{1}$$

$$\varepsilon_{re} = (\varepsilon_r + 1)/2 \tag{2}$$

where l_1 and l_2 are the lengths of the ground plane and radiation patch, respectively; g is the gap between the ground plane and radiating patch; A_1 and A_2 are the ground plane and radiation patch area, respectively; ε_{re} is the effective dielectric constant.

In the literature, various shapes of monopole elements have been proposed for the design of UWB-MIMO antennas such as square [24], rectangle [25], and triangle [26]. The size of the radiating element should be large enough to achieve a lower cutoff frequency of 3.1 GHz for designing a UWB antenna while keeping compactness. Slots often enhance the current path in radiating elements [27]. Various antennas have been designed using U-shaped structures for wideband applications in the existing literature [28–30]. In this article, a U-shaped radiating element is designed by cutting a rectangular slot in rectangle-shaped monopole antenna elements. The effect of width (denoted by symbol "A" in Figure 1) of U-shaped radiating elements is studied for the optimization of the proposed UWB-MIMO antenna. The effect of the width of U-shaped radiating elements on simulated S_{11} parameters is shown in Figure 3. With width $(A) = 1.5$ mm, there is better return-loss at lower and higher frequencies than other values of width (A) of U-shaped monopole elements due to better impedance matching. The current path length changes as the width varies, and the conductor area is also reduced to minimize the losses and hence the opportunity to have better matching obtained at the lower and the higher frequencies. A

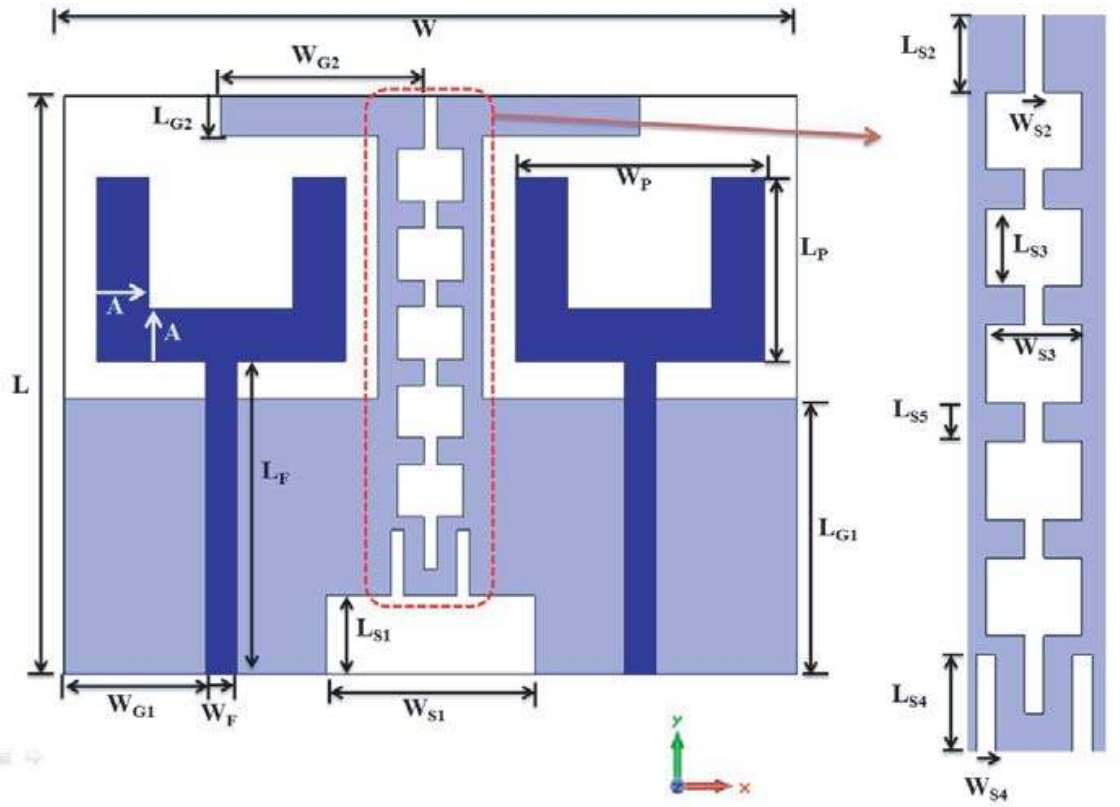

Figure 1. Proposed fractal UWB-MIMO antenna (dark blue: upper surface, light blue: bottom surface).

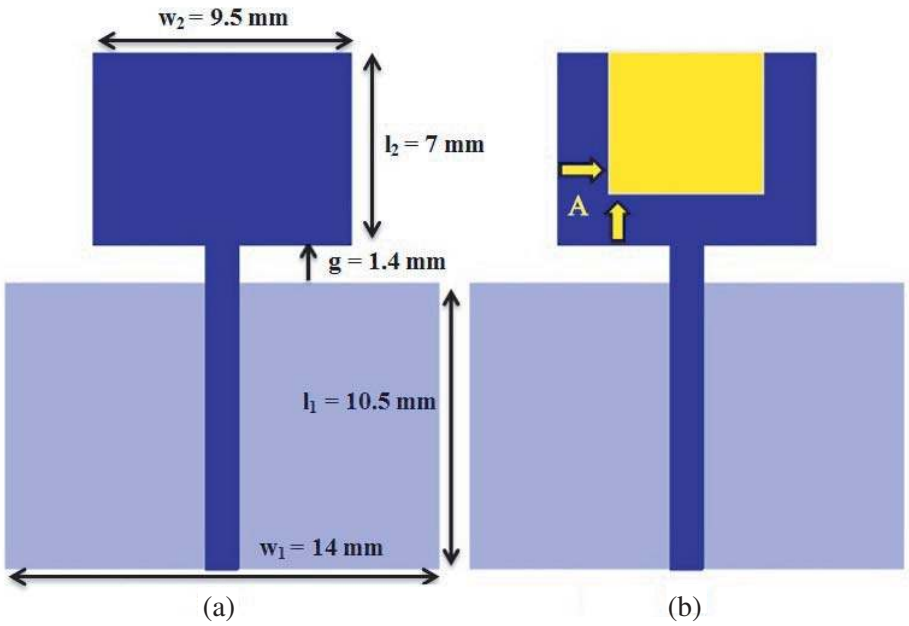

Figure 2. Evolution of U-shaped monopole element. (a) Rectangular shaped. (b) U-shaped (dark blue: upper surface, light blue: bottom surface, yellow: slot in upper surface).

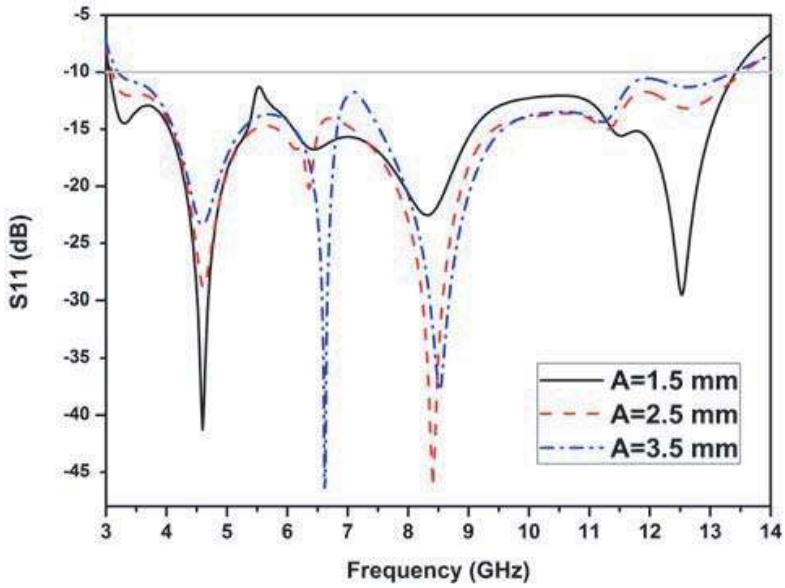

Figure 3. Simulated S_{11}-parameters against frequency for the different values of width (A) of U-shaped monopole elements of MIMO antenna while other parameters are the same as listed in Table 2.

novel modified Minkowski fractal shaped slot is loaded in the ground plane between radiating elements of this antenna to increase the isolation. This antenna is simulated using CST Microwave Studio.

2.2. Effect of Novel CMMF

The term fractal originally devised by Benoit Mandelbrot [31]. Fractal geometry carries self-similar and self-affine properties [16, 31]. Fractal can be used in antennas to increase miniaturization and to create multiband and wideband properties [32]. The isolation can be enhanced by using fractals in MIMO antennas [22]. A novel modified Minkowski fractal structure at iteration-1 is generated by iterated function system (IFS), and it is shown in Figure 4(a). Its mirror image fractal structure is shown in Figure 4(b). These fractal structures, as shown in Figure 4(a) and Figure 4(b), are joined together by keeping 0.5 mm separation between them. Then, this novel complementary Minkowski fractal structure is vertically placed between U-shaped monopole elements, as shown in Figure 1. The IFS transformation coefficients of the proposed novel fractal structure (Figure 4(a)) are given in Table 3. The IFS technique is used to generate a fractal structure, and it is described by matrix Equation (3) shown in [33–35]. This method is based on the concept of a series of affine transformations (W) that is defined by

$$W\begin{bmatrix} x \\ y \end{bmatrix} = \begin{bmatrix} a & b \\ c & d \end{bmatrix}\begin{bmatrix} x \\ y \end{bmatrix} + \begin{bmatrix} e \\ f \end{bmatrix} \tag{3}$$

where matrix elements (a, b, c, d) are responsible for scaling and rotation, and (e, f) are responsible for linear translation concerning the x-axis and y-axis in coordinate systems.

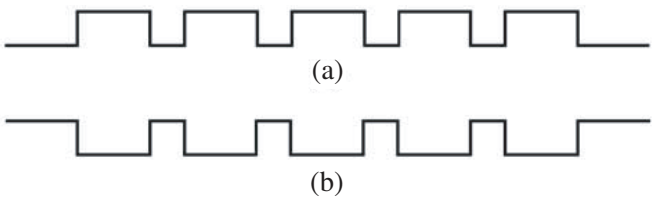

Figure 4. (a) Proposed novel modified Minkowski fractal structure at iteration-1. (b) Mirror image of the proposed structure.

Table 3. IFS transformation coefficients for the proposed structure.

W	a	b	c	d	e	f
1	1/9	0	0	1/9	0	0
2	0	−1/18	1/18	0	1/9	0
3	1/9	0	0	1/9	1/9	1/18
4	0	1/18	−1/18	0	2/9	1/18
5	1/18	0	0	1/18	2/9	0
6	0	−1/18	1/18	0	5/18	0
7	1/9	0	0	1/9	5/18	1/18
8	0	1/18	−1/18	0	7/18	1/18
9	1/18	0	0	1/18	7/18	0
10	0	−1/18	1/18	0	4/9	0
11	1/9	0	0	1/9	4/9	1/18
12	0	1/18	−1/18	0	5/9	1/18
13	1/18	0	0	1/18	5/9	0
14	0	−1/18	1/18	0	11/18	0
15	1/9	0	0	1/9	11/18	1/18
16	0	1/18	−1/18	0	13/18	1/18
17	1/18	0	0	1/18	13/18	0
18	0	−1/18	1/18	0	7/9	0
19	1/9	0	0	1/9	7/9	1/18
20	0	1/18	−1/18	0	8/9	1/18
21	1/9	0	0	1/9	8/9	0

DGSs are used to reduce mutual coupling between radiating elements of MIMO antennas [36–39]. It disturbs and diverts the surface current distribution and suppresses the coupled fields between the radiating elements of the MIMO antenna [40]. The evolution process of the ground plane for the proposed MIMO antenna is shown in Figure 5. DGSs disturb the surface current distribution in the ground plane, which is responsible for the coupling of current among antennas when they are closely placed, say significantly less than $\lambda/2$. To redistribute the surface current or decouple the path, we etch some part of the ground plane to alter the distribution of surface current and try to majorly restrict them to the respective antenna elements rather than getting coupled to the nearby antenna elements. In our case, DGSs do not affect the resonating frequency but help in improving the isolation, achieving lower values of the transmission coefficient, as shown in Figure 6. The same concept has been strengthened

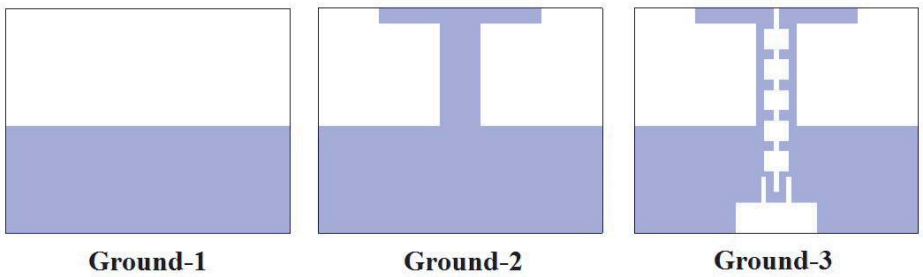

Figure 5. Evolution structures of the ground plane.

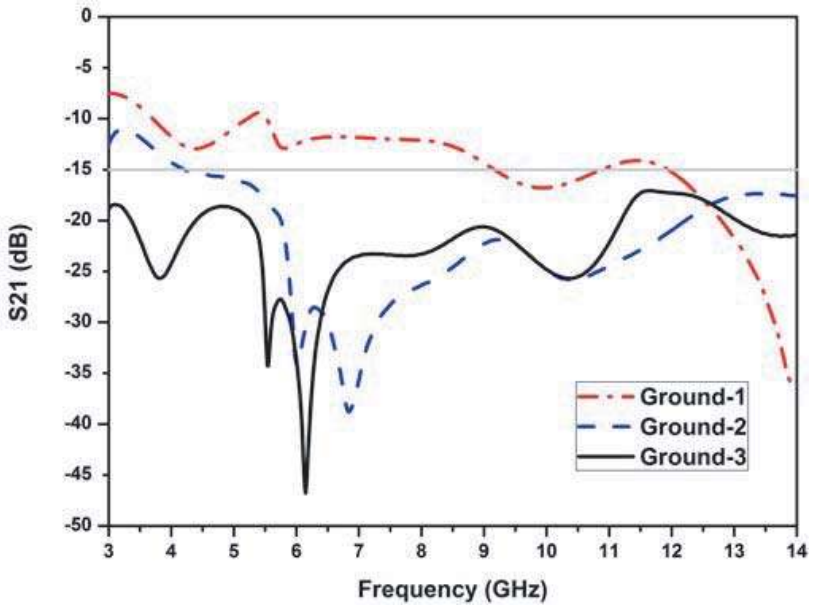

Figure 6. Mutual coupling, S_{21} parameters for the different ground configurations.

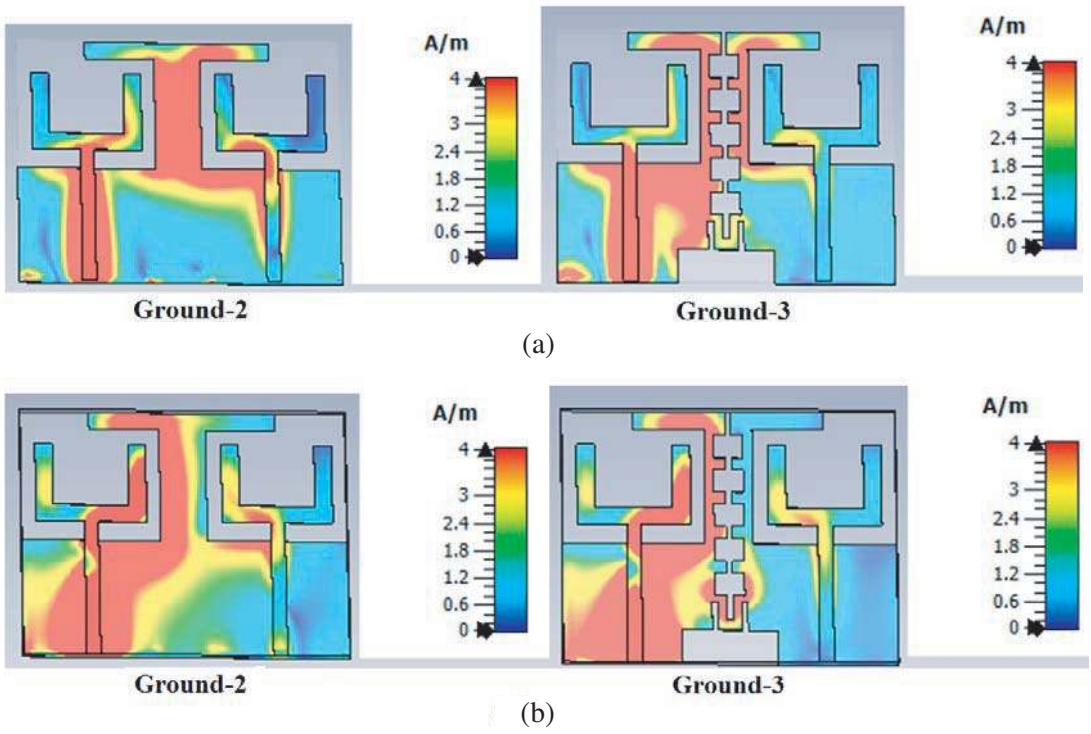

Figure 7. Surface current distributions without and with CMMF while port-1 is excited, and port-2 is terminated at (a) 3.1 GHz, (b) 4.5 GHz.

through the surface current distribution and electric field distribution shown in Figures 7 and 8 where we can find higher concentration on the other antenna element before introducing the novel isolation structure between them.

For Ground-1, the mutual coupling, S_{21}, is above -15 dB for almost the entire UWB frequency

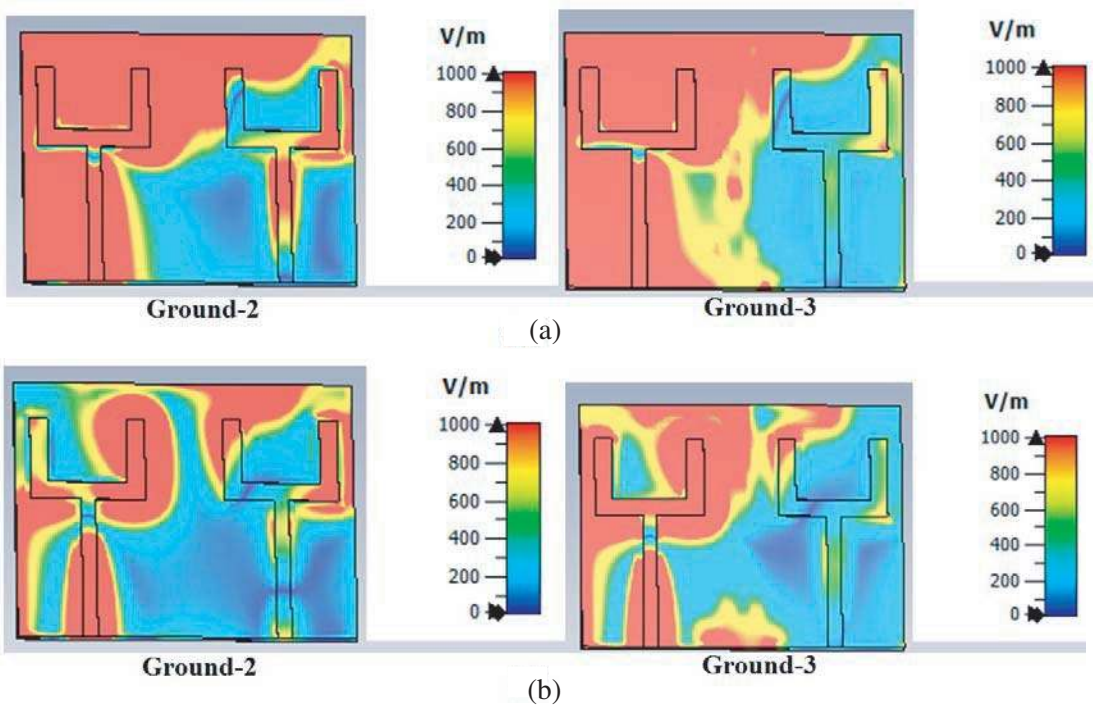

Figure 8. Electric field distributions without and with CMMF while port-1 is excited and port-2 is terminated at (a) 3.1 GHz, (b) 4.5 GHz.

range. The mutual coupling, S_{21}, should be less than -15 dB between radiating elements of MIMO antennas [25]. T-shaped ground enhances isolation [41]. Hence, we used a T-shaped ground stub (Ground-2) to reduce mutual coupling between U-shaped radiating elements of the proposed MIMO antenna. The mutual coupling, S_{21}, is suppressed below -15 dB for the entire UWB frequency range except the frequency band ranging from 3.0 to 4.2 GHz. But we need to design an antenna for UWB applications. Therefore, we introduced a novel modified Minkowski fractal shaped slot in the ground plane and a rectangular slot at bottom (Ground-3) to enhance the isolation for the entire UWB frequency range from 3.1 to 10.6 GHz. Ground-3 suppressed the mutual coupling, S_{21} below -17.07 dB for the entire operating bandwidth and -18.4 dB for the UWB frequency range 3.1 to 10.6 GHz. U-shaped radiating elements MIMO antenna with Ground-3 configuration can be used for UWB applications.

The effects of the introduction of CMMF in the ground plane on surface current and E-field distributions at two different resonant frequencies 3.1 GHz and 4.5 GHz are shown in Figures 7(a) and (b). Figure 7 shows the surface current distribution keeping first port excited and second port terminated with a 50 Ω matched load. It is observed that a sufficient amount of current is coupled near CMMF. Thus, CMMF reduced coupled current density near the second U-shaped monopole element of the UWB-MIMO antenna. The structure is also helpful in suppressing space wave propagation, as we have observed in Figures 8(a) and (b) that the E-field distributions inside the substrate are restricted from one antenna element to another in the case of Ground-3 as compared to Ground-2.

3. RESULTS AND DISCUSSION

The U-shaped UWB-MIMO antenna with novel CMMF for isolation enhancement is fabricated, and its prototype image is shown in Figure 9. The measured S-parameters are determined using the Keysight vector network analyzer (Model N9916A). The simulated and measured S-parameters of the proposed MIMO antenna are shown in Figure 10. It is observed in Figure 10 that there is good agreement between simulated and measured S-parameters of the proposed UWB-MIMO antenna. There is little variation between results due to fabrication limitations, environmental losses, and SMA connectors.

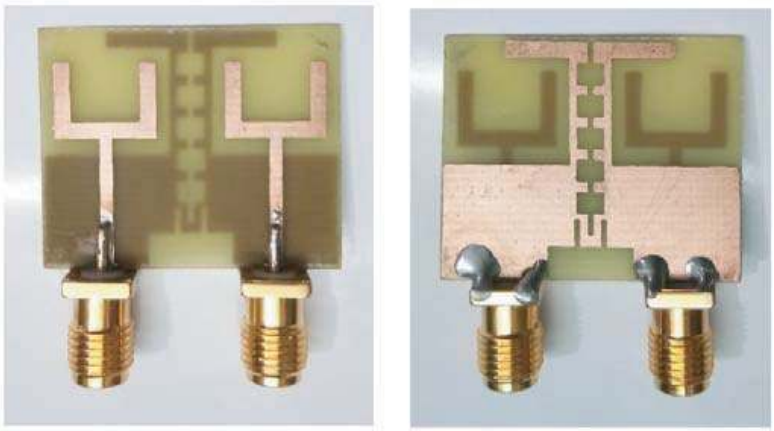

(a) (b)

Figure 9. Prototype of the proposed antenna. (a) Front. (b) Back.

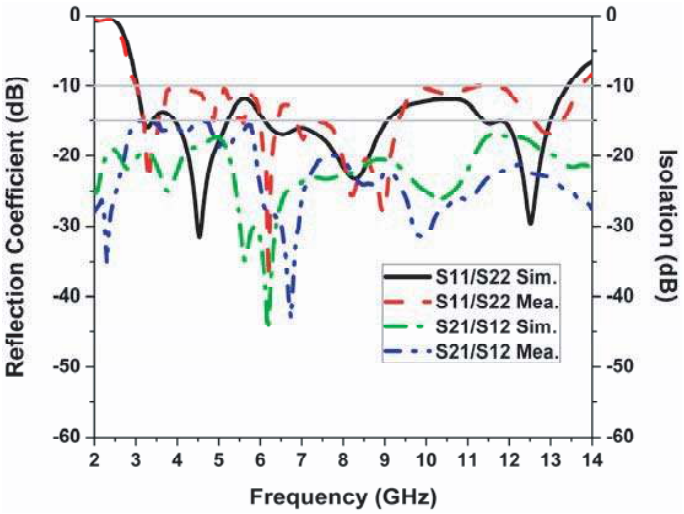

Figure 10. S-parameter analysis of the proposed antenna.

In Figure 10, we can find that the isolation is more than 15 dB for the entire range, where the reflection coefficient is below −10 dB. The impedance bandwidth is 10.35 GHz (3.06 GHz to 13.41 GHz), and fractional bandwidth is 125.68% for the proposed U-shaped UWB-MIMO antenna. The value of minimum isolation is 17.07 dB for the entire operating impedance bandwidth and 18.4 dB for UWB frequency range 3.1 GHz to 10.6 GHz. The image of the anechoic chamber is shown in Figure 11, where the measurement of the radiation pattern is done. A normalized radiation pattern is illustrated in Figure 12, where we can observe that an almost omnidirectional radiation pattern is achieved in E-plane (XZ-plane) at all the given frequencies except a few distortions at 12.50 GHz after taking both the ports into considerations. The cross-polarisation effect has also been shown at different frequencies, and it is observed that the isolation is more than 20 dB from the co-polarisation radiation pattern at various angles of elevation including the main lobe direction in both the E-plane (XZ-plane) and H-plane (YZ-plane) which confirms that the proposed MIMO antenna is linearly polarised.

The plot of maximum gain against frequency is plotted in Figure 13, where we can observe almost a flat gain of 2 dBi from 3 to 10.5 GHz. There is an exponential rise of gain up to 6 dBi as the operating frequency increases from 10.5 GHz to 13.5 GHz. As we can see from the radiation pattern given in Figure 12, the antenna becomes more directive at 12.50 GHz, which is one of the reasons for the exponential rise in the maximum gain attained as the frequency increases.

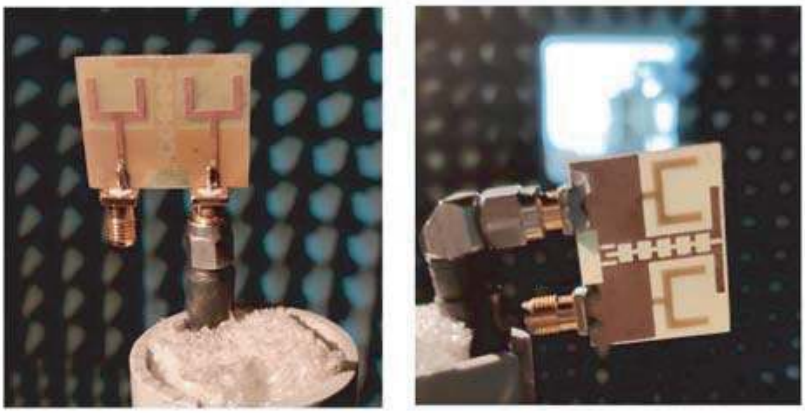

(a) (b)

Figure 11. Measurement setup in the anechoic chamber. (a) XZ-plane measurement (E-plane). (b) YZ-plane measurement (H-plane).

4. DIVERSITY PERFORMANCE

Diversity performance of the MIMO antenna helps in defining its diverse performance of individual antenna elements of a MIMO system in rich scattering and multi-path fading environment.

$$\rho_{ij} = \frac{\left|\int \Omega \left[XPR \cdot E_{\theta i} E^*_{\theta j} P_\theta + E_{\phi i} E^*_{\phi j} P_\phi\right] d\Omega\right|^2}{\int \Omega \left\{XPR \cdot E_{\theta i} E^*_{\theta i} P_\theta + E_{\phi i} E^*_{\phi i} P_\phi\right\} d\Omega \times \int \Omega \left\{XPR \cdot E_{\theta j} E^*_{\theta j} P_\theta + E_{\phi j} E^*_{\phi j} P_\phi\right\} d\Omega} \tag{4}$$

$$DG = 10 \times e_p = 10 \times \sqrt{(1 - \rho_e^2)} \tag{5}$$

Envelope Correlation Coefficient (ECC) defines how closely one antenna element, i.e., the ith antenna element, is correlated to another antenna, i.e., the jth antenna element in a MIMO system. The ECC can be defined using S-parameters [14] and far-field distributions [16]. While the S-parameters approach defines only port isolation, the far-field approach defines the correlation among the far-field radiation patterns and hence helps in defining spatial diversity rather than only port diversity. So, the ECC has been computed using Equation (4) from the far-field radiation pattern keeping Cross-Polarisation Ratio, $XPR = 1$. We can find that the ECC is below 0.05 for the entire operating frequency range as shown in Figure 14.

Diversity gain (DG) is the performance factor to characterize a diversity system. DG is dependent on the correlation coefficient, and it can be calculated by using Equation (5) as given in [42]. Here, e_p is the diversity gain reduction factor due to the correlation between the two antenna elements. The diversity gain is above 9.98 dB for the entire operating frequency as shown in Figure 14.

$$MEG = \int_0^{2\pi} \int_0^{\pi} \left[\frac{XPR}{1 + XPR} G_\theta(\theta, \phi) P_\theta(\theta, \phi) + \frac{1}{1 + XPR} G_\phi(\theta, \phi) P_\phi(\theta, \phi)\right] \sin\theta d\theta d\phi \tag{6}$$

Mean Effective Gain (MEG) is the ratio of average power received to the incident power by any antenna elements in a MIMO system as compared to an isotropic antenna in a fading environment [4]. The computed MEG for $XPR = 1$ from the far-field power and gain radiation pattern is shown in Figure 15. It is observed that the MEG is below -3 dB, and also the criteria $|MEG_i - MEG_j| < \pm 3$ dB for excellent diversity performance have been fulfilled.

$$TARC = \frac{\sqrt{|S_{11} + S_{12}e^{j\theta}|^2 + |S_{21} + S_{22}e^{j\theta}|^2}}{\sqrt{2}} \tag{7}$$

Another important diversity parameter is the Total Active Reflection coefficient (TARC), which states the non-variance of the average of the S-parameters characteristics of the MIMO antenna system

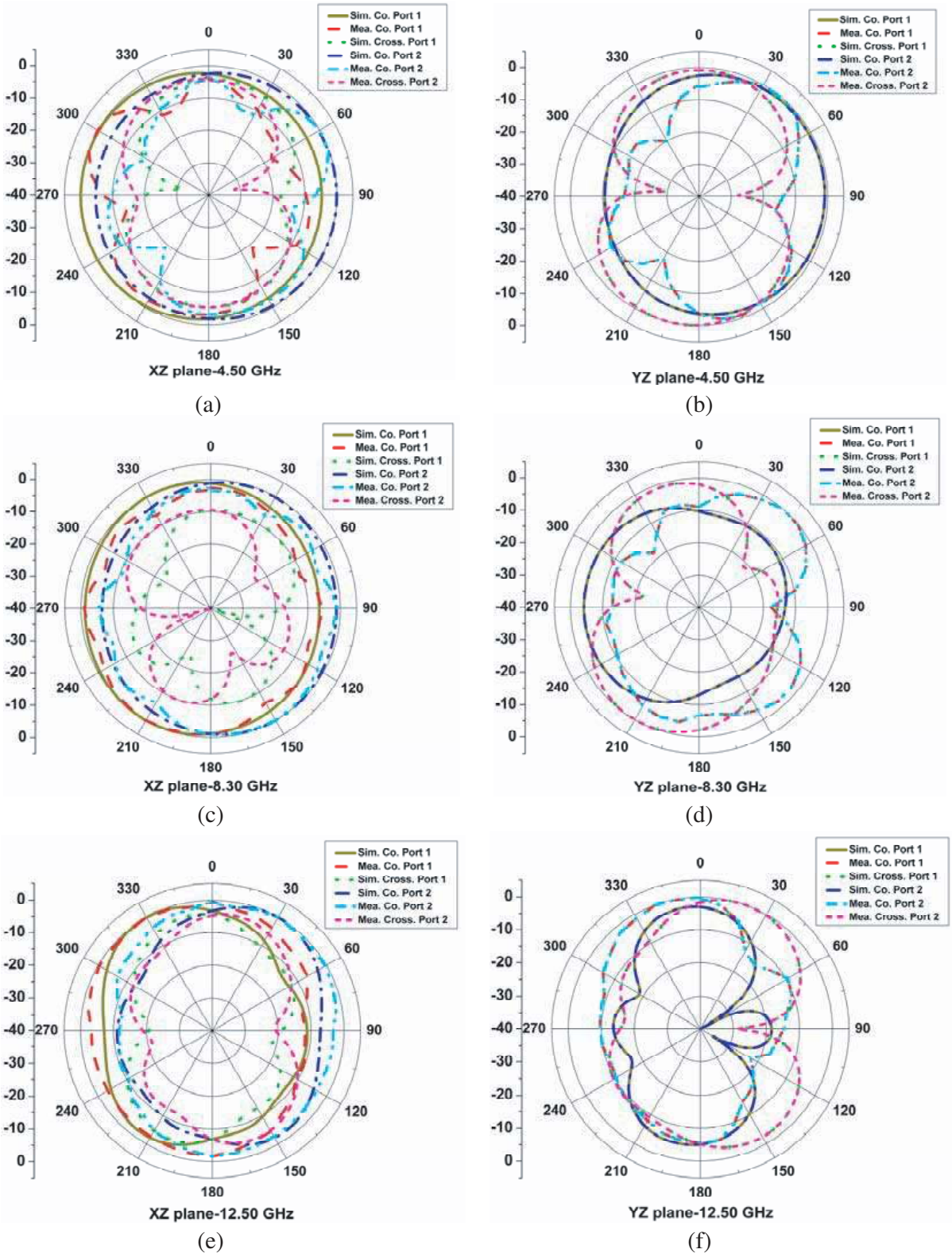

Figure 12. Normalized co- and cross-polarization far-field radiation pattern in both E and H-plane. (a) XZ-plane-4.50 GHz, (b) YZ-plane-4.50 GHz, (c) XZ-plane-8.30 GHz and (d) YZ-plane-8.30 GHz, (e) XZ-plane-12.50 GHz, (f) YZ-plane-12.50 GHz.

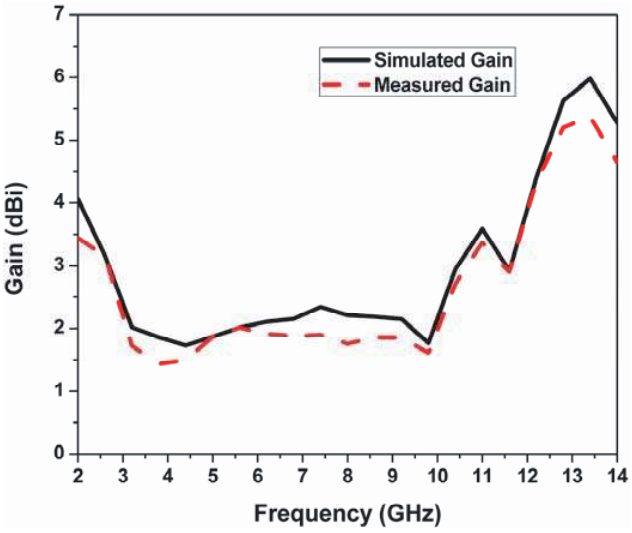

Figure 13. Gain measurement vs frequency.

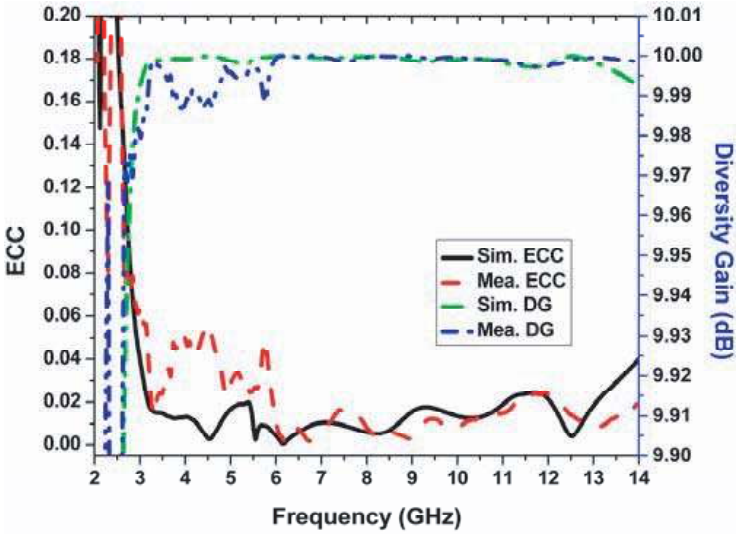

Figure 14. ECC & DG analysis.

even when the phase of the input signal of one of the antenna elements is kept changing as compared to another antenna element. The computed TARC from the S-parameters results with Equation (7) [4, 43] shown in Figure 16 illustrates that the proposed structure follows the reflection coefficient despite the phase variation of the input signal at the ports from 30° to 180°.

At last, Channel Capacity Loss (CCL) is computed, which helps in defining the loss of transmission bits/s/Hz in a high data rate transmission. The minimum acceptable limit of CCL over which the high data transmission is feasible is defined by 0.4 bits/s/Hz [14, 44]. The measured CCL is computed using Equation (8) against frequency, shown in Figure 17, where it is found as low as 0.3 bits/s/Hz as required for the successful operation of the MIMO antenna.

$$C_{loss} = -\log_2 \det\left(\alpha^R\right) \tag{8}$$

where,

$$\alpha^R = \begin{bmatrix} \alpha_{11} & \alpha_{12} \\ \alpha_{21} & \alpha_{22} \end{bmatrix}, \quad \alpha_{11} = 1 - \left(|S_{11}|^2 + |S_{12}|^2\right), \quad \alpha_{22} = 1 - \left(|S_{22}|^2 + |S_{21}|^2\right),$$

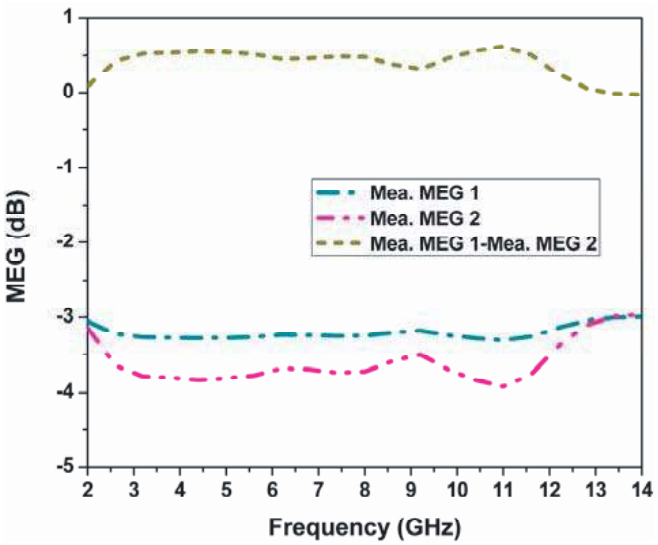

Figure 15. Mean Effective Gain measurement.

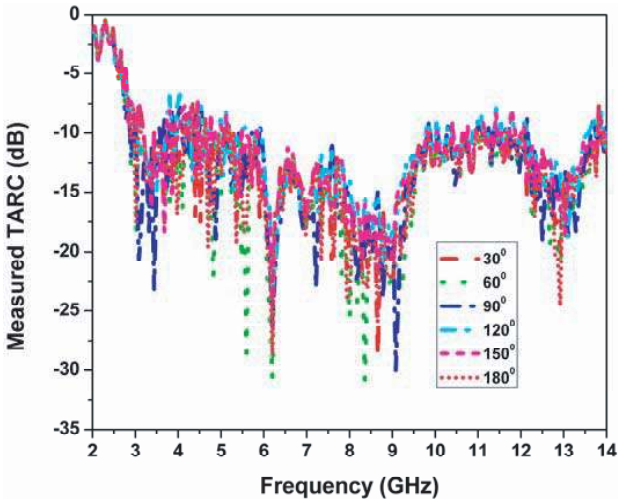

Figure 16. TARC measurement.

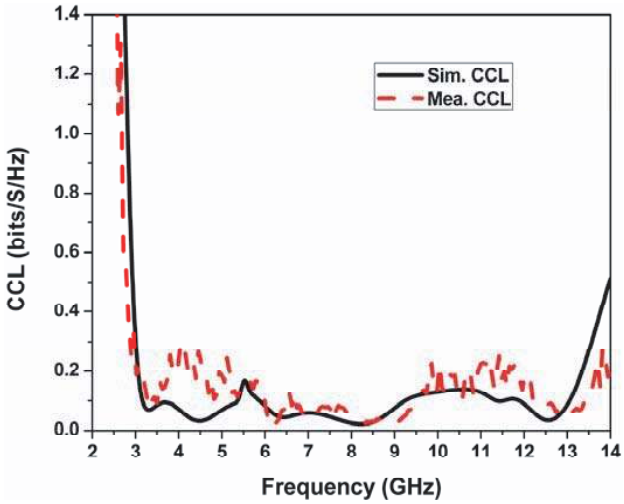

Figure 17. CCL measurement.

$$\alpha_{12} = -\left(S_{11}^{*}S_{12} + S_{21}^{*}S_{12}\right), \quad \alpha_{21} = -\left(S_{22}^{*}S_{21} + S_{12}^{*}S_{21}\right)$$

5. CONCLUSIONS

A compact U-shaped UWB-MIMO antenna with novel complementary modified Minkowski fractal for isolation enhancement is proposed having dimensions $22 \times 28 \times 0.8\,\text{mm}^2$. This antenna is fabricated on an FR-4 substrate and investigated experimentally. The proposed MIMO antenna is designed using two U-shaped monopole elements for the UWB operations with impedance bandwidth of 10.35 GHz ranging from 3.06 GHz to 13.41 GHz and fractional bandwidth of 125.68%. A novel CMMF structure is introduced in the ground plane between the U-shaped monopole elements for the isolation enhancement better than 17.07 dB for the entire operating impedance bandwidth while 18.4 dB for UWB frequency range 3.1 GHz to 10.6 GHz. Almost a flat gain of 2 dBi is for UWB range (3–10.5 GHz), which exponentially rises to 6 dBi at the higher frequency 13.5 GHz. The measured ECC and CCL are less

than 0.05 and 0.3 b/s/Hz, respectively, for the entire operating bandwidth of the proposed antenna. Other diversity performance parameters results are also found satisfactory. So all these results advocate that the proposed novel and compact MIMO antenna is suitable for UWB applications.

REFERENCES

1. Federal Communications Commission, "Federal Communications Commission revision of Part 15 of the commission's rules regarding ultra-wideband transmission system from 3.1 to 10.6 GHz," ET-Docket, 98–153, Washington, DC, USA, 2002.
2. Bolin, T., A. Derneryd, G. Kristensson, V. Plicanic, and Z. Ying, "Two-antenna receive diversity performance in indoor environment," *IEEE Electron. Lett.*, Vol. 41, No. 2, 1205–1206, 2005.
3. Mabrouk, I. B., L. Talbi, M. Nedil, and K. Hettak, "MIMO-UWB channel characterization within an underground mine gallery," *IEEE Trans. Antennas Propag.*, Vol. 60, No. 10, 4866–4874, 2012.
4. Kumar, A., A. Q. Ansari, B. K. Kanaujia, and J. Kishor, "A novel ITI-shaped isolation structure placed between two-port CPW-fed dual-band MIMO antenna for high isolation," *AEU — International Journal of Electronics and Communications*, Vol. 104, 35–43, 2019.
5. Nadeem, I. and D. Choi, "Study on mutual coupling reduction technique for MIMO antennas," *IEEE Access*, Vol. 7, 563–586, 2019.
6. Li, Y., X. Yang, C. Liu, and T. Jiang, "Miniaturization cantor set fractal ultrawideband antenna with a notch band characteristic," *Microw. Opt. Technol. Lett.*, Vol. 54, No. 5, 1227–1230, 2012.
7. Werner, D. H., R. L. Haupt, and P. L. Werner, "Fractal antenna engineering: The theory and design of fractal antenna arrays," *IEEE Antennas and Propag. Mag.*, Vol. 41, No. 5, 37–58, 1999.
8. Anguera, J., C. Puente, C. Borja, and J. Soler, "Fractal-shaped antennas: A review," *Encyclopedia of RF and Microwave Engineering*, Wiley, Hoboken, NJ, Vol. 2, 1620-1635, 2005.
9. Haji-Hashemi, M. R., H. M. M. Sadeghi, and V. M. Moghtadai, "Space-filling patch antennas with CPW feed," *Progress In Electromagnetics Research*, Vol. 2, 69–73, 2006.
10. Azari, A., "A new ultra-wideband fractal monopole antenna," *Int. J. Electron.*, Vol. 99, 295–303, 2012.
11. Banerjee, J., R. Ghatak, and A. Karmakar, "A compact planar UWB MIMO diversity antenna with Hilbert fractal neutralization line for isolation improvement and dual band notch characteristics," *Emerging Trends in Electronic Devices and Computational Techniques (EDCT)*, 1–6, Kolkata, 2018.
12. Banerjee, J., A. Karmakar, and R. Ghatak, "A compact printed UWB MIMO monopole antenna with modified complementary fractal for isolation improvement and triple band notch characteristics," *2018 Fifteenth International Conference on Wireless and Optical Communications Networks (WOCN)*, 1–5, Kolkata, 2018.
13. Tripathi, S., A. Mohan, and S. Yadav, "A compact octagonal fractal UWB MIMO antenna with WLAN band rejection," *Microw. Opt. Technol. Lett.*, Vol. 57, 1919–1925, 2015.
14. Gurjar, R., D. K. Upadhyay, B. K. Kanaujia, and K. Sharma, "A novel compact self-similar fractal UWB MIMO antenna," *Int. J. RF Microw. Comput. Aided Eng.*, e21632, 2018.
15. Sohi, A. K. and A. Kaur, "A complementary Sierpinski gasket fractal antenna array integrated with a complementary Archimedean defected ground structure for portable 4G/5G UWB MIMO communication devices," *Microw. Opt. Technol. Lett.*, Vol. 62, 2595–2605, 2020.
16. Gurjar, R., D. K. Upadhyay, B. K. Kanaujia, and A. Kumar, "A compact modified Sierpinski carpet fractal UWB MIMO antenna with square-shaped funnel-like ground stub," *AEU — International Journal of Electronics and Communications*, Vol. 117, 153126, 2020.
17. Sampath, R. and K. T. Selvan, "Compact hybrid Sierpinski Koch fractal UWB MIMO antenna with pattern diversity," *Int. J. RF Microw. Comput. Aided Eng.*, e22017, 2019.
18. Tripathi, S., A. Mohan, and S. Yadav, "A compact Koch fractal UWB MIMO antenna with WLAN band-rejection," *IEEE Antennas Wireless Propag. Lett.*, Vol. 14, 1565–1568, 2015.
19. Rajkumar, S., A. Amala Anto, and K. T. Selvan, "Isolation improvement of UWB MIMO antenna utilizing molecule fractal structure," *Electronics Letters*, Vol. 55, No. 10, 576–579, 2019.

20. Rajkumar, S., K. T. Selvan, and P. H. Rao, "Compact 4 element Sierpinski Knopp fractal UWB MIMO antenna with dual band notch," *Microw. Opt. Technol. Lett.*, Vol. 60, 1023–1030, 2018.
21. Gorai, A., A. Dasgupta, and R. Ghatak, "A compact quasi-self-complementary dual band notched UWB MIMO antenna with enhanced isolation using Hilbert fractal slot," *AEU — International Journal of Electronics and Communications*, Vol. 94, 36–41, 2018.
22. Banerjee, J., A. Karmakar, R. Ghatak, and D. R. Poddar, "Compact CPW-fed UWB MIMO antenna with a novel modified Minkowski fractal Defected Ground Structure (DGS) for high isolation and triple band-notch characteristic," *Journal of Electromagnetic Waves and Applications*, Vol. 31, No. 15, 1550–1565, 2017.
23. Thomas, K. G. and M. Sreenivasan, "A simple ultrawideband planar rectangular printed antenna with band dispensation," *IEEE Trans. Antennas Propag.*, Vol. 58, No. 1, 27–34, 2010.
24. Toktas, A., M. Yerlikaya, K. Sabanci, et al., "Reducing mutual coupling for a square UWB MIMO antenna using various parasitic structures," *10th International Conference on Electrical and Electronics Engineering (ELECO)*, 982–986, Bursa, 2017.
25. Liu, L., S. W. Cheung, and T. I. Yuk, "Compact MIMO antenna for portable devices in UWB applications," *IEEE Trans. Antennas Propag.*, Vol. 61, No. 8, 4257–4264, 2013.
26. Zhang, S., Z. Ying, J. Xiong, and S. He, "Ultrawideband MIMO/diversity antennas with a tree-like structure to enhance wideband isolation," *IEEE Antennas Wireless Propag. Lett.*, Vol. 8, 1279–1282, 2009.
27. Chandel, R., A. K. Gautam, and K. Rambabu, "Design and packaging of an eye-shaped multiple-input-multiple-output antenna with high isolation for wireless UWB applications," *IEEE Transactions on Components, Packaging and Manufacturing Technology*, Vol. 8, No. 4, 635–642, 2018.
28. Mandal, K. and P. P. Sarkar, "High gain wide-band U-shaped patch antennas with modified ground planes," *IEEE Transactions on Antennas and Propagation*, Vol. 61, No. 4, 2279–2282, 2013.
29. Elhabchi, M., M. N. Srifi, and R. Touahni, "A novel modified U-shaped microstrip antenna for Super Wide Band (SWB) applications," *Analog. Integr. Circ. Sig. Process.*, Vol. 105, 571–578, 2020.
30. Mishra, S. K. and J. Mukherjee, "WLAN band-notched printed U-shape UWB antenna," *International Conference on Signal Processing and Communications (SPCOM)*, 1–5, Bangalore, 2012.
31. Mandelbrot, B. B., *The Fractal Geometry of Nature*, W. H. Freeman, New York, 1983.
32. Haji-Hashemi, M. R., H. M. M. Sadeghi, and V. M. Moghtadai, "Space-filling patch antennas with CPW feed," *Progress In Electromagnetics Research Symposium*, Vol. 2, 69–73, 2006.
33. Sinha, S. N. and M. Jain, "A self-affine fractal multiband antenna," *IEEE Antennas Wireless Propag. Lett.*, Vol. 6, 110–112, 2007.
34. Gurjar, R., R. Singh, and S. Kumar, "Elliptically slotted self-affine 8-shaped fractal multiband antenna," *Proceedings of the Int. Conf. on Recent Cognizance in Wireless Comm. & Image Processing Springer*, 783–789, Jaipur, India, 2016.
35. Gurjar, R., D. K. Upadhyay, and B. K. Kanaujia, "Compact four-element 8-shaped self-affine fractal UWB MIMO antenna," *IEEE International Microwave and Photonics Conference Preceedings*, 1–2, Dhanbad, India, 2018.
36. Khandelwal, M. K., B. K. Kanaujia, and S. Kumar, "Defected ground structure: Fundamentals, analysis, and applications in modern wireless trends," *Int. J. Antennas Propag.*, Vol. 2017, 1–22, Article ID 2018527, 2017.
37. Webster, J. G., M. S. Bhuiyan, and N. C. Karmakar, "Defected ground structures for microwave applications," *Wiley Encyclopedia of Electrical and Electronics Engineering*, J. G. Webster (ed.), Jan. 2014.
38. Weng, L. H., Y. C. Guo, X. W. Shi, and X. Q. Chen, "An overview on defected ground structure," *Progress In Electromagnetics Research B*, Vol. 7, 173–189, 2008.

39. Breed, G., "An introduction to defected ground structures in microstrip circuits. High frequency electronics," *Summit Technical Media*, 50–54, 2008.
40. Sharawi, M. S., *Printed MIMO Antenna Engineering*, Artech House, Norwood, MA, USA, 2014.
41. Liu, L., S. W. Cheung, and T. I. Yuk, "Compact MIMO antenna for portable UWB applications with band-notched characteristic," *IEEE Trans. Antennas Propag.*, Vol. 63, No. 5, 1917–1924, 2015.
42. Dkiouak, A., A. Zakriti, M. E. Ouahabi, and A. Mchbal, "Design of two element Wi-MAX/WLAN MIMO antenna with improved isolation using a Short Stub-Loaded Resonator (SSLR)," *Journal of Electromagnetic Waves and Applications*, Vol. 34, No. 9, 1268–1282, 2020.
43. Rekha, V. S. D., P. Pardhasaradhi, B. T. P. Madhav, and Y. U. Devi, "Dual-band notched orthogonal 4-element MIMO antenna with isolation for UWB applications," *IEEE Access*, Vol. 8, 145871–145880, 2020.
44. Sultan, K. S. and H. H. Abdullah, "Planar UWB MIMO-diversity antenna with dual notch characteristics," *Progress In Electromagnetics Research C*, Vol. 93, 119–129, 2019.